Journal of Alloys and Compounds 693 (2017) 565–572

Contents lists available at ScienceDirect

Journal of Alloys and Compounds

journal homepage: http://www.elsevier.com/locate/jalcom

Role of ion species in radiation effects of $Lu_2Ti_2O_7$ pyrochlore

Dongyan Yang [a, b], Yue Xia [a], Juan Wen [a], Jinjie Liang [a, b], Pengcheng Mu [a], Zhiguang Wang [b], Yuhong Li [a, *], Yongqiang Wang [c]

[a] School of Nuclear Science and Technology, Lanzhou University, Lanzhou 730000, China
[b] Institute of Modern Physics, Chinese Academy of Sciences, Lanzhou 730000, China
[c] Materials Science and Technology Division, Los Alamos National Laboratory, Los Alamos, NM 87545, USA

ARTICLE INFO

Article history:
Received 16 July 2016
Received in revised form
12 September 2016
Accepted 20 September 2016
Available online 21 September 2016

Keywords:
Radiation effects
Ion species
Pyrochlores
Amorphization
Lattice swelling

ABSTRACT

In an attempt to investigate the role of ion species in the radiation effects of pyrochlores, polycrystalline $Lu_2Ti_2O_7$ samples, prepared through a standard solid state process, were irradiated with three different ion beams: 400 keV Ne^{2+}, 2.7 MeV Ar^{11+} and 6.5 MeV Xe^{26+}. To characterize the damaged layers in $Lu_2Ti_2O_7$, the grazing incident X-ray diffraction technique was applied. All the three irradiations induce significant amorphization processes and lattice swelling in $Lu_2Ti_2O_7$. However, when the ion fluence is converted to a standard dose in dpa, the radiation effects of $Lu_2Ti_2O_7$ show a great dependence on the implanted ion species. The threshold amorphization dose decreases with increasing ion mass and energy. Besides, the amorphization rate, as well as lattice swelling rate, increases with increasing ion mass and energy. That is, the $Lu_2Ti_2O_7$ pyrochlore is more susceptible to amorphization and lattice swelling under heavier ion irradiation. These results are then discussed in the framework of defect configuration and the density of collision cascades based on Monte Carlo simulations.

1. Introduction

Global expansion of nuclear power has been proposed as an excellent solution to the problems associated with increasing energy use, excessive dependence on fossil fuels and greenhouse gas emissions [1–4]. However, the management of increasing radioactive wastes becomes one of the important concerns in the development of nuclear power. The safe immobilization of toxic nuclear wastes, including minor actinides (U, Np, Th, Am and Cm) in spent nuclear fuel and Pu from dismantled nuclear weapons, is a major challenge facing humanity today. Currently, ceramic materials, which can survive in the extreme environment of radiation, are proposed as potential matrices for the disposal of high-level radioactive wastes [3–6].

The pyrochlores with formula of $A_2B_2O_7$ (A = Rare earths, B = Zr, Ti, Sn and Hf) are promising ceramic host phases for the immobilization of actinides [7–9]. $A_2B_2O_7$ pyrochlores belong to $Fd\bar{3}\ m$ space group, and have a superstructure of the well-known fluorite structure ($Fm\bar{3}\ m$). The unit cell contains eight molecules (Z = 8) and four crystallographically nonequivalent sites. As the origin is fixed on B site, atoms occupy the following special positions: A at 16*d* (0.5, 0.5, 0.5), B at 16*c* (0, 0, 0), O at 48*f* (*x*, 0.125, 0.125) and 8*b* (0.375, 0.375, 0.375). The 8*a* site is unoccupied. Among these coordinates, only the 48*f* oxygen position parameter (*x*) is changeable. Both the cations and the anion vacancies are ordered on the cation and anion sublattice respectively, and the pyrochlore can be regarded as an ordered defective fluorite structure.

Extensive studies have been devoted to the radiation effects of titanate and zirconate pyrochlores irradiated with various ion beams [9–23]. Pyrochlores generally undergo significant structural evolution under ion irradiations, including amorphization [10,17], order-to-disorder phase transformation [24], lattice swelling [12,25,26] and phase separation [12]. The factors that govern the radiation tolerance of pyrochlores are quite complex, mainly involving the 48*f* oxygen positional parameter (*x*) [10], the radius ratio of A- to B-cation [21–23], the defect energetics [27–30], the ionicity of chemical bonds [14,31], the formation enthalpy [32], as well as the inherent atomic disorder [13,18]. First principles calculations have shown that the cation antisite defect is the most energetically favorable defect in $Sm_2Ti_2O_7$, $Gd_2Ti_2O_7$ and $Lu_2Ti_2O_7$ pyrochlores [25,29]. However, a molecular dynamics simulation investigation [33] shows that it is the cation Frenkel pair defect rather than the cation antisite defect that contributes to the amorphization in $Gd_2Ti_2O_7$ [10].

* Corresponding author.
E-mail address: liyuhong@lzu.edu.cn (Y. Li).

http://dx.doi.org/10.1016/j.jallcom.2016.09.227
0925-8388/

From the perspective of implanted ions, the mass and energy are critical factors which determine the energy deposition of the ions and thereby the damage build-up in target materials [34,35]. The effects of ion species have been mentioned in various experimental studies [9,36], including materials such as $Cd_2Nb_2O_7$, $Gd_2Ti_2O_7$, $Lu_2Ti_2O_7$, $Ca_2La_8(SiO_4)_6O_2$ and 6H-SiC, where the efforts were mainly focused on the critical amorphization temperatures and recovery activation energies. However, the discrepancy of radiation effects of materials under different ion irradiations was not well understood yet, which correlates the results of ion beam irradiation experiments to the radiation damage induced by α- and β-events in nuclear waste matrices. Herein, we report on a systematic study of the influence of ion species (400 keV Ne^{2+}, 2.7 MeV Ar^{11+} and 6.5 MeV Xe^{26+}) on the radiation behavior of $Lu_2Ti_2O_7$.

2. Experimental details

Polycrystalline $Lu_2Ti_2O_7$ samples were prepared via a standard solid state process. Stoichiometric amounts of Lu_2O_3 (99.99% pure) and TiO_2 (99.99% pure) were intimately mixed using a ball-mill. The powders were subsequently pressed into pellets at the pressure of ~400 MPa. The compacts were first sintered at 1200 °C for 24 h. To attain better homogeneity, the procedures (grinding, milling and pressing) were repeated with a second heating at 1450 °C for 48 h. The resulted pellets were then polished to a mirror finish.

$Lu_2Ti_2O_7$ samples were irradiated with three ion species with different masses and energies. The 400 keV Ne^{2+} ion irradiations were carried out at cryogenic temperature (~77 K) using a 200 kV Danfysik high current research ion implanter in the Ion Beam Materials Laboratory at Los Alamos National Laboratory, and the 2.7 MeV Ar^{11+} and 6.5 MeV Xe^{26+} ion irradiations were performed at room temperature (~293 K) on a 320 kV platform for multi-discipline research with highly charged ions at the Institute of Modern Physics, Chinese Academy of Sciences (CAS). All the ions were implanted at normal incidence. The ion fluences for different irradiations are listed in Table 1. The flux of each ion irradiation is significantly low ($\leq 1 \times 10^{12}$ ions/(cm^2·s)), and thus the flux effect was neglected in the following discussion section.

To estimate the ranges, energy deposition and displacement damages of each ion irradiation, the ion transport Monte Carlo simulations were performed using the SRIM (Stopping and Range of Ions in Matter) code with the Full Damage Cascades mode [37]. In these simulations, the threshold displacement energies for Lu, Ti and O atom were set as 84, 205 and 52 eV respectively, as calculated for $Gd_2Ti_2O_7$ pyrochlore [38]. The ion projected range of 400 keV Ne ions is ~0.40 μm, which is much smaller than those of 2.7 MeV Ar and 6.5 MeV Xe ion (1.19 and 1.25 μm respectively). Fig. 1 shows the variation of displacement damage as a function of depth under each irradiation at the fluence of 1×10^{15} ions/cm^2. The maximum peak displacement damages at fluence of 1×10^{15} ions/cm^2 are approximately 0.20, 0.35 and 1.39 dpa (displacements per atom) for Ne, Ar and Xe irradiation respectively. According to this result, the ion fluence (in ions/cm^2) of each irradiation was converted into a standard damage dose (in dpa) for ease of comparison among different ion species, as presented in Table 1. Table 1 also gives the ion projected range (R_p), as well as the nuclear (S_n) and electronic (S_e) energy loss.

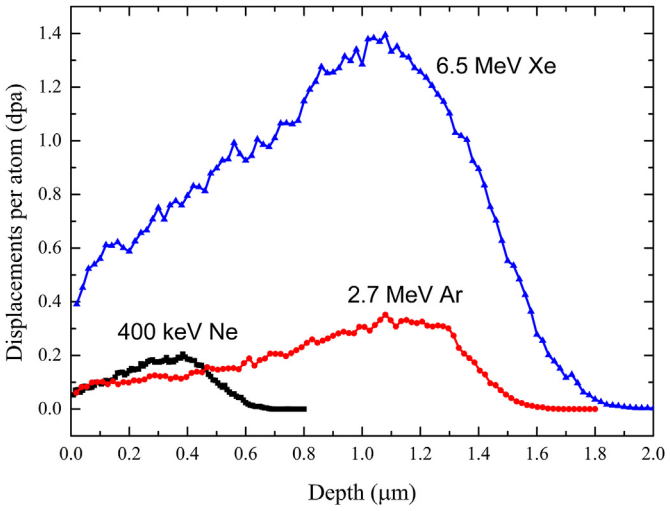

Fig. 1. Variation of the displacement damage vs. depth in $Lu_2Ti_2O_7$ for 400 keV Ne, 2.7 MeV Ar and 6.5 MeV Xe ion implantations at fluence of 1.0×10^{15} ions/cm^2.

Ion irradiation induced structural damage was characterized by grazing incident X-ray diffraction (GIXRD) method. For $Lu_2Ti_2O_7$ samples irradiated with 400 keV Ne^{2+} ions, please see Ref. [25]. For $Lu_2Ti_2O_7$ samples irradiated with 2.7 MeV Ar^{11+} and 6.5 MeV Xe^{26+} ions, the X-ray incidence angle was $\gamma = 1°$. The scan range of 2θ is from 10° to 70°, with a step of 0.02° and a dwell time of 1 s. The incident angles chosen here can ensure that only radiation damaged layers were detected by X-rays.

3. Results

Fig. 2 displays the normalized GIXRD patterns of $Lu_2Ti_2O_7$ samples before and after 400 keV Ne^{2+} (a), 2.7 MeV Ar^{11+} (b) and 6.5 MeV Xe^{26+} (c) irradiations, illustrating the structural evolution with increasing ion dose. For the pristine $Lu_2Ti_2O_7$ (see the bottom pattern in Fig. 2(a)), each diffraction peak can be referred to the pyrochlores structure, as labeled with the Miller indices. Actually two series of diffraction peaks are observed. The first series with high intensities contains the peaks corresponding to the parent fluorite structure, as marked with even Miller indices (such as (2 2 2), (4 0 0) and (4 4 0)). The second series with low intensities, as marked with odd Miller indices (such as (1 1 1), (3 1 1) and (3 3 1)), corresponds to the superstructure of the ordered $A_2B_2O_7$ pyrochlore. The XRD pattern reveals that pristine $Lu_2Ti_2O_7$ samples

Table 1
The irradiation parameters for each irradiation on $Lu_2Ti_2O_7$.

Ion species	R_p (μm)	S_n[a]	S_e[a]	Irradiation fluences and doses					
		keV/nm							
400 keV Ne^{2+}	0.40	0.15	0.68	Fluence (ions/cm^2)	0	7×10^{14}	1×10^{15}	2×10^{15}	4×10^{15}
				Dose (dpa)	0	0.14	0.20	0.40	0.80
2.7 MeV Ar^{11+}	1.19	0.22	1.88	Fluence (ions/cm^2)	0	2×10^{14}	4×10^{14}	6×10^{14}	8×10^{14}
				Dose (dpa)	0	0.07	0.14	0.21	0.28
6.5 MeV Xe^{26+}	1.25	1.20	3.45	Fluence (ions/cm^2)	0	2×10^{13}	3.5×10^{13}	5×10^{13}	1.2×10^{14}
				Dose (dpa)	0	0.03	0.05	0.07	0.17

[a] The mean values of nuclear and electronic energy loss within the range from the implanting surface to the depth of displacement damage peak.